

Calculations of the Free Energy of Interaction of the c-Fos–c-Jun Coiled Coil: Effects of the Solvation Model and the Inclusion of Polarization Effects

Zhili Zuo,[†] Neha S. Gandhi,[†] and Ricardo L. Mancera*,^{†,‡}

Curtin Health Innovation Research Institute, Western Australian Biomedical Research Institute, School of Biomedical Sciences and School of Pharmacy, Curtin University, GPO Box U1987, Perth WA 6845, Australia

Received August 23, 2010

The leucine zipper region of activator protein-1 (AP-1) comprises the c-Jun and c-Fos proteins and constitutes a well-known coiled coil protein–protein interaction motif. We have used molecular dynamics (MD) simulations in conjunction with the molecular mechanics/Poisson–Boltzmann generalized-Born surface area [MM/PB(GB)SA] methods to predict the free energy of interaction of these proteins. In particular, the influence of the choice of solvation model, protein force field, and water potential on the stability and dynamic properties of the c-Fos–c-Jun complex were investigated. Use of the AMBER polarizable force field ff02 in combination with the polarizable POL3 water potential was found to result in increased stability of the c-Fos–c-Jun complex. MM/PB(GB)SA calculations revealed that MD simulations using the POL3 water potential give the lowest predicted free energies of interaction compared to other nonpolarizable water potentials. In addition, the calculated absolute free energy of binding was predicted to be closest to the experimental value using the MM/GBSA method with independent MD simulation trajectories using the POL3 water potential and the polarizable ff02 force field, while all other binding affinities were overestimated.

INTRODUCTION

Protein–protein interactions mediate most cellular processes, such as signal transduction, gene regulation, and cell division,^{1–3} and their imbalance is often associated with numerous diseases, such as cancer and diabetes.^{4,5} One of the most abundant protein interaction domains is the coiled coil motif⁶ consisting of two or more α -helices wrapped around each other to form a left-handed supercoil. Coiled coils play major roles in a variety of biological processes, such as cell signaling, DNA transcription, cell division, viral infection, fertilization, and force generation. Coiled coil sequences are usually denoted as $(a-b-c-d-e-f-g)_n$ in one helix and $(a'-b'-c'-d'-e'-f'-g')_n$ in the other, as it consists of 3.5 residues for every turn, while a conserved seven-residue repeat occurs every two turns of the coiled coil helix (Figure 1).^{6,7} Despite their apparent simple domain structure and dimerization interface, coiled coils have highly specific homo- and heterotypic interactions. Hydrophobic amino acids typically make up the dimerization interface between the helices, and the other amino acids in the heptad are mostly polar or charged and can form inter- and intrahelical interactions that contribute to the stability and the specificity of the dimerization.^{8,9}

Understanding the mechanism of interaction of coiled coil proteins and how to interfere with it is of great importance in biology and medicine as part of efforts to develop therapeutic agents, diagnostics, and analytical tools. Structure determinations, thermodynamic measurements, and mutagenesis studies have greatly contributed to the current under-

standing of coiled coil interactions, especially the properties of binding interfaces of homo/heterocomplexes. Despite much progress on the determination of the stability of coiled coil structures by protein design, protein cloning, atomic force microscopy (AFM), circular dichroism (CD), and size-exclusion chromatography (SEC),^{10–12} only a few theoretical studies using computational methods have been used to predict the stability^{11,13–17} or the binding affinity of coiled coil structures.^{15,18}

Estimating coiled coil interaction energies using an atomistic-level approach remains a challenging problem. In addition to the linear interaction energy (LIE)^{19,20} and linear response approximation (LRA)^{21,22} methods, the molecular mechanics/Poisson–Boltzmann surface area (MM/PBSA) and the molecular mechanics generalized Born surface area (MM/GBSA) methods are also popular rapid computational approaches used to predict the free energy of interaction of biomolecules from molecular dynamics (MD) simulation trajectories in reasonably good agreement with experiment,^{23–28} although in some cases they tend to overestimate the experimental value.²⁹ The MM/PBSA method typically involves the calculation of the molecular mechanics gas-phase energies, continuum electrostatic solvation energies (by solving the linearized Poisson–Boltzmann equation), surface area-based nonpolar energies, and entropic terms from normal modes calculations.^{29,30} Compared to MM/PBSA, MM/GBSA is a faster method in which the electrostatic contribution to the solvation free energy is approximated by the GB model. Both of these methods give efficient, reproducible, and reliable calculations.

Polarizable and nonpolarizable force fields differ in their treatment of electrostatic interactions, with most polarizable models accounting for polarization using the inducible point dipole model, the classical Drude oscillator model, or the

* Corresponding author. E-mail: r.mancera@curtin.edu.au. Telephone: +61 8 92661017.

[†] School of Biomedical Sciences.

[‡] School of Pharmacy.

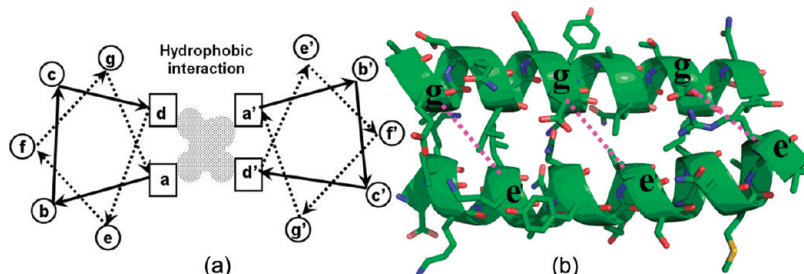


Figure 1. Structure and interactions in a dimeric parallel coiled coil (modified from Mason et al.). (a) Helical wheel diagram (looking down from the N-terminus to the C-terminus). Heptad residue positions are labeled a–g and a'–g'. (b) Side view of part of the coiled coil domain of the human c-Fos–c-Jun complex, shown as ribbons (PDB code: 1FOS). The hydrogen-bond or ionic interactions between residues in positions g and e' are shown with dotted lines, and the hydrophobic interactions between residues in positions a, d and a', d' are indicated by the gray region in the middle of diagram A.

fluctuating charge model.^{31,32} The polarizable AMBER force field (ff02 with the POL3 water potential) has been reported to perform better than its nonpolarizable counterpart (ff03 with the TIP3P water potential) in calculations of the free energy of binding of ligand–DNA complexes,³³ although other reports suggest that the nonpolarizable force field ff99SB with the TIP4P-Ew water potential can better reproduce experimental structures and dynamic properties^{34,35} and can accurately predict free energies of binding of biotin analogues to avidin.³⁶ On the other hand, it has been reported that the use of force fields ff99SB and ff03 with the TIP3P water potential can describe better the stability of coiled coil structures compared to the ff94, ff96, and ff99 force fields.¹⁵ Therefore, it remains unclear whether the inclusion of polarization effects in the protein force field and/or water potential results in a better representation of coiled coil structures and interactions.

We have chosen to investigate the accuracy of MD simulations using the MM/PBSA and MM/GBSA methods for the prediction of the free energy of binding of the protein–protein coiled coil interaction in the oncoprotein heterodimer c-Jun–c-Fos, which constitutes the leucine zipper region in the transcription factor activator protein-1 (AP-1). In particular, we have compared the predicted free energies of binding derived from MD simulations using polarizable (AMBER ff02 in combination with the POL3 water potential) and nonpolarizable (AMBER ff99SB with TIP3P, TIP4P, and TIP4P-Ew water potentials) force fields. The polarizable and nonpolarizable versions of the AMBER force field differ from each other primarily in their treatment of electrostatic interactions, whereby the polarizable version includes an explicit treatment of induction effects using dipole polarizabilities on all atoms.

MATERIALS AND METHODS

Protein Structure Preparation. The crystal structure of the c-Fos–c-Jun complex (PDB entry: 1FOS) was used to provide reference atomic coordinates and modified to reflect the amino acid sequence reported by Arndt et al. Residues Ser177 in c-Fos and Ser301 in c-Jun were mutated to tyrosine.^{11,12} They estimated the free energy of binding of the c-Fos–c-Jun complex to be -17.1 kJ/mol using CD determinations. Terminal residues were capped with an ACE (acetyl beginning group) and NME (*N*-methylamine ending group) in the N- and C-terminus, respectively. The amino acid sequence used for c-Fos is thus ASTDTLQAETDQLE-DEKYALQTEIANLLKEKEKLGAP, while that of c-Jun is

ASIASRLEEKVKTTLKAQNYELASTANMLREQVAQLGAP. Separate structures for c-Fos and c-Jun were extracted directly from the above structure of their heterodimer. Residues Lys, Arg, Glu, and Asp were kept ionized during the simulations by assuming a neutral pH.

MD Simulations. All energy minimizations and MD simulations were performed using the AMBER 9.0 program with the nonpolarizable ff99SB³⁷ and polarizable ff02^{38,39} force fields. Cubic boxes of TIP3P,⁴⁰ TIP4P-Ew,⁴¹ or TIP4P water molecules were used to solvate the protein complex in combination with the nonpolarizable force field or of POL3⁴² water molecules with the polarizable force field.

In all cases a minimum distance of 12.0 Å was kept between each face of the box and the protein, resulting in the addition of 5700–5800 water molecules. Net charges in each system were neutralized by adding an appropriate number of counterions (Na^+ or Cl^-). In all simulations the particle mesh Ewald (PME) method was used to compute long-range electrostatic interactions,⁴³ using a 1.0 Å grid spacing and a fourth-order spline for interpolation. The nonbonded cutoff was set to 10.0 Å, and the SHAKE algorithm⁴⁴ was used to constrain all bonds involving hydrogen atoms. All simulations were carried out in the isobaric–isothermal (NPT) ensemble. Isotropic scaling of the pressure was used with an external pressure of 1 atm using weak coupling to a pressure bath.⁴⁵ The temperature was kept at 293 K (which is the reference temperature of the CD determinations) using Langevin dynamics⁴⁶ with a collision frequency of 2 ps^{-1} . A time step of 1.0 fs was used in all simulations. Periodic boundary conditions were applied throughout.

Initial unfavorable steric contacts with the solvent or within the protein molecules were removed by energy minimization. Initially 10 000 steps of energy minimization (5000 steps of steepest descents and 5000 steps of conjugate gradients) were carried out in which a restraining force (41.8 kJ/mol·Å²) was applied to all protein atoms, after which another 10 000 steps of energy minimization were carried out in which the same restraining force was applied to all backbone atoms only, and finally another 10 000 steps of energy minimization were carried out without any restraining force. The systems were then heated from 0 to 293 K over 50 ps under constant volume and temperature conditions (NVT). Constant pressure and temperature (NPT) simulations were then used to equilibrate the system at 1 atm and 293 K over 50.0 ps, while applying a weak restraining force (20.9 kJ/mol·Å²) to the whole protein, followed by a further 50.0 ps with the same

restraining force applied only on all backbone atoms, and then finally 25.0 ps without any restraints. At this point the systems were deemed to have equilibrated. The production phases of the simulations were then run without any restraints at 293 K for 10 ns for each protein system. Various properties (density, temperature, pressure, kinetic and potential energies) were monitored during the simulations, and snapshots were saved every 10 ps. Overall, simulations carried out using the polarizable ff02/POL3 combination took almost twice as long as simulations using the ff99SB/TIP3P combination, with the other simulations using ff99SB, and either TIP4P or TIP4P/Ew took intermediate times to complete.

To investigate whether conformational changes during the simulations may affect the calculation of the free energy of binding, both single and independent-trajectory approaches were used. In the single-trajectory approach, a single simulation of the coiled coil complex was performed, whereby the coordinates of the complex and each protein within the complex were extracted along the simulation to calculate the free energy of binding. In the independent-trajectory approach, separate simulations were carried out for the protein complex and for each of the proteins, so that the coordinates of each protein system were extracted from independent simulations to calculate the free energy of binding. To enhance the exploration of conformational phase space,³⁶ 10 independent 1.0 ns trajectories of the protein complex were also obtained by running MD simulations with different initial velocities on the same starting protein structure by using a different random seed number to initialize velocities according to a Maxwell distribution.

The root mean squared deviation (rmsd) between the initial coordinates of the backbone atoms of the proteins and the coordinates along the MD simulations was computed for every snapshot. The total α -helicity of the proteins was calculated employing the defined secondary structure of proteins (DSSP) definitions, whereby helicity was taken as the number of helical residues determined by DSSP.⁴⁷ Helical propensity was taken as the percentage helicity of all amino acid residues.

Free Energy Calculations. The MM/PBSA and MM/GBSA methods were used to compute the free energies of binding from the snapshots collected during the simulations. The decomposition of the free energy into additive contributions from various force field terms and/or different groups of atoms is substantiated by rigorous derivations in the free energy perturbation (FEP) formalism.^{48,49} In the MM/PB(GB)SA method, the free energy of a given complex is calculated by summing up the molecular mechanics energies, solvation energies, and entropic terms, according to the equation:

$$G = E_{\text{MM}} + G_{\text{PBSA}} - \text{TS} \quad (1)$$

where E_{MM} is the average molecular mechanics energy, calculated as

$$E_{\text{MM}} = E_{\text{int}} + E_{\text{vdw}} + E_{\text{elec}} \quad (2)$$

where $E_{\text{int}} = E_{\text{bond}} + E_{\text{angle}} + E_{\text{tors}}$. E_{int} corresponds to the sum of the average internal bond stretching, bond bending, and torsional angle energies. E_{vdw} is the average van der Waals energy, and E_{elec} is the average electrostatic energy.

G_{PBSA} is the free energy of solvation, given by

$$G_{\text{PBSA}} = G_{\text{PB}} + G_{\text{SA}} \quad (3)$$

where G_{PB} is the electrostatic component of the free energy of solvation, calculated by solving the Poisson–Boltzmann equation in the MM/PBSA method (or the generalized Born equation in the case of the MM/GBSA method).⁵⁰ G_{SA} is the nonpolar contribution to the free energy of solvation, which is calculated from the solvent-accessible surface area (SASA).⁵¹ This term is computed with the equation $G_{\text{SA}} = \gamma \text{SA} + \beta$, where SA is the solvent-accessible surface area (calculated, for example, by the MSMS program),⁵² and γ and β are parametrized constants. A total of 500 snapshots were extracted every 20 ps from each 10.0 ns simulation trajectory for these calculations.

The final term, TS, is the sum of translational, rotational, and vibrational entropies. The translational and rotational entropies are approximated by statistical mechanics equations of molecules in the gas phase. The vibrational entropy is approximated by performing a normal modes calculation. A total of 250 snapshots were extracted every 40 ps from each 10.0 ns simulation trajectory for these analyses.

The free energy of binding ΔG for the association of two molecules is thus calculated as

$$\Delta G = G_{\text{complex}} - G_{\text{molecule1}} - G_{\text{molecule2}} \quad (4)$$

MM/PBSA calculations were carried out using the PBSA module,⁵³ and MM/GBSA calculations were carried out using the Sander module within the AMBER 9.0 program.^{37,54}

RESULTS AND DISCUSSION

In this study we have investigated the influence of the solvation model (PB vs GB) and the inclusion of polarization effects in both the protein force field and the water potential on the calculation of the free energy of binding of the coiled coil c-Fos–c-Jun complex.

Structural Stability of the c-Fos–c-Jun Complex. To assess the stability of the coiled coil structure of the c-Fos–c-Jun complex, the running average (the cumulative average at any point in time during the simulation) of the rmsd of all backbone atoms of the complex and each separate protein was calculated with respect to the initial structure. Rmsd data for all backbone atoms in all simulations can be found in Figures S1 and S2 in the Supporting Information. Plots of the running average rmsd of the c-Fos–c-Jun complex, c-Fos peptide, and c-Jun peptide during single-trajectory, independent-trajectory, and multiple short-trajectory MD simulations are shown in Figure 2. The overall average rmsd for each MD simulation approach and force field and the water potential combination used are reported in Table 1.

To determine if the differences in rmsd are statistically significant, paired sample t tests were carried out between each force field/water potential combination. All differences in rmsd were determined to be statistically significantly different at $\alpha = 0.01$.

The lowest average rmsd (1.82 Å) was obtained with the ff02/POL3 combination over a 10.0 ns single-trajectory approach simulation, with increasingly higher values of the average rmsd for the ff99SB/TIP3P, ff99SB/TIP4P-Ew, and ff99SB/TIP4P combinations. When using multiple short-

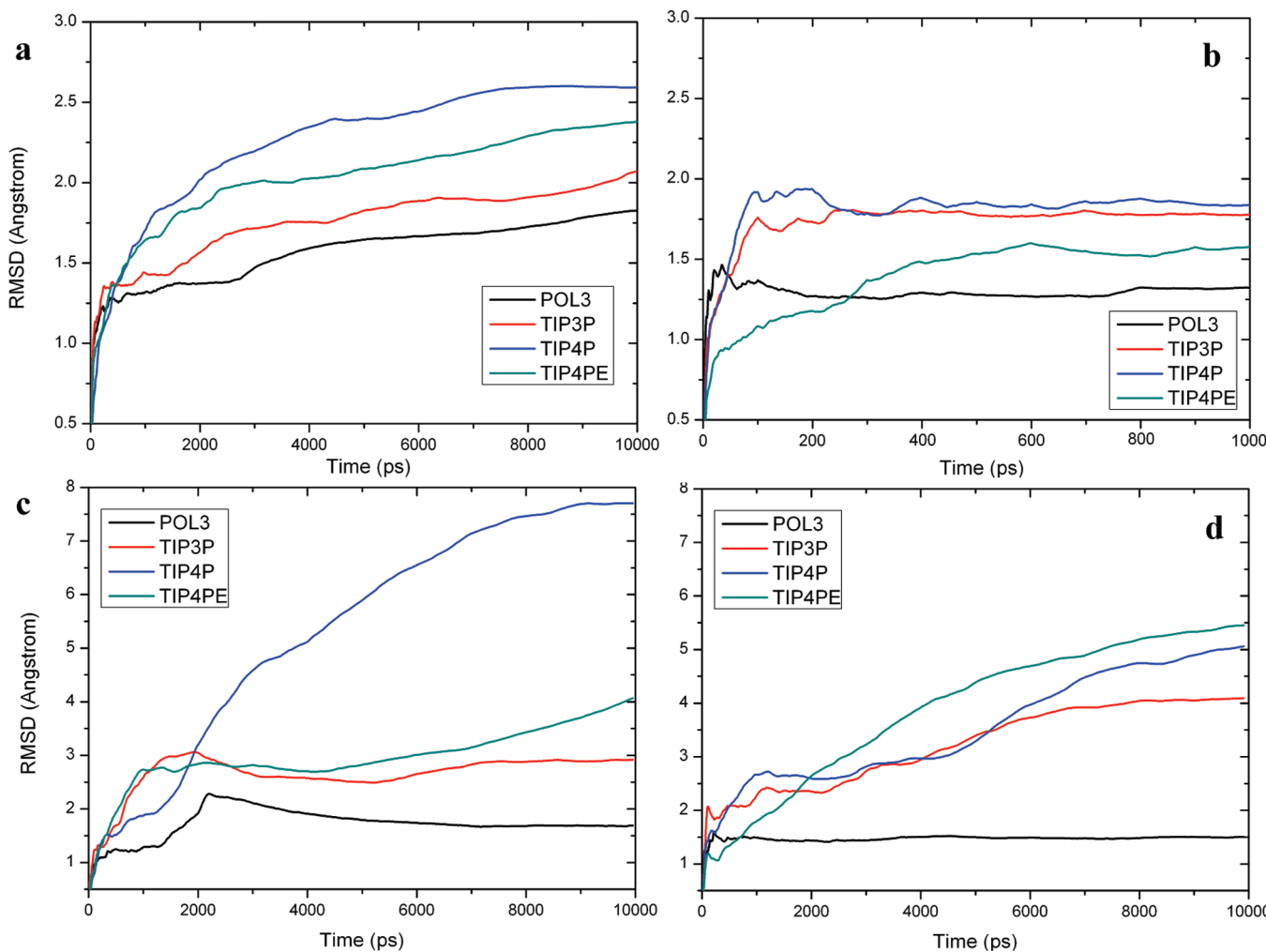


Figure 2. Plots of the running average of the rmsd calculated for all backbone atoms during MD simulations with different protein force fields and water potentials: (a) Rmsd values of the c-Fos–c-Jun complex in the single-trajectory approach simulation; (b) rmsd of the c-Fos–c-Jun complex averaged over 10 short-trajectory simulations; (c) rmsd values of the c-Fos peptide in the independent-trajectory approach simulation; and (d) rmsd values of the c-Jun peptide in the independent-trajectory approach simulation. For simplicity, only the name of the water potential is shown in the labels for each curve.

Table 1. Average Rmsd for Each MD Simulation Approach for Each Combination of Protein Force Field and Water Potential

protein force field/water potential			independent trajectories	
	single trajectory	multiple short trajectories	c-Fos	c-Jun
ff99SB/TIP3P	2.07	1.78	2.93	4.11
ff99SB/TIP4P	2.59	1.84	7.70	5.08
ff99SB/TIP4P-Ew	2.38	1.58	4.09	5.46
ff02/POL3	1.82	1.32	1.69	1.61

trajectory approach simulations, the lowest average rmsd (1.32 \AA) was also obtained with the ff02/POL3 combination, with higher (and similar) average rmsd values for the other protein force field/water potential combinations.

It can be seen in Figure 2a that several nanoseconds are required for the protein complexes in all single-trajectory approach simulations to begin to reach a relative stable conformation. The simulation with the ff02/POL3 combination appears to stabilize more rapidly than the other simulations with other potentials. On the other hand, the running average of the rmsd in the simulations appears to reach a lower, stable value after averaging over 10 short, independent simulations (multiple-trajectory approach, Figure 2b), and this occurs after only 2–3 ns. This behavior is to be expected

from short simulations where all conformations are still relatively close to the starting conformation.

It is interesting to note that in the simulations of each peptide on their own (Figure 2c and d), the running average of the rmsd rapidly reached a lower, stable value when using the ff02/POL3 combination, whereas the rmsd tended to increase significantly during most of the simulation time in all the other nonpolarizable combinations. It is also surprising that the ff99SB/TIP4P resulted in a notoriously larger increase in the rmsd of the c-Fos peptide (Figure 2c), although all simulations of the peptides on their own using nonpolarizable combinations resulted in large increases in rmsd, suggesting that the peptides are not stable in these simulations (see further below). Rmsd values in the independent-trajectory approach using all nonpolarizable force field/water potential combinations are much higher than those obtained in the single-trajectory approach. This indicates that the peptides on their own in solution are significantly less stable than in the complex. However, simulations using the polarizable ff02/POL3 combination reveal that the peptides are equally stable both on their own and in their complex. Similar observations have been reported in simulations of HIV protease, where the overall structural fluctuations of the

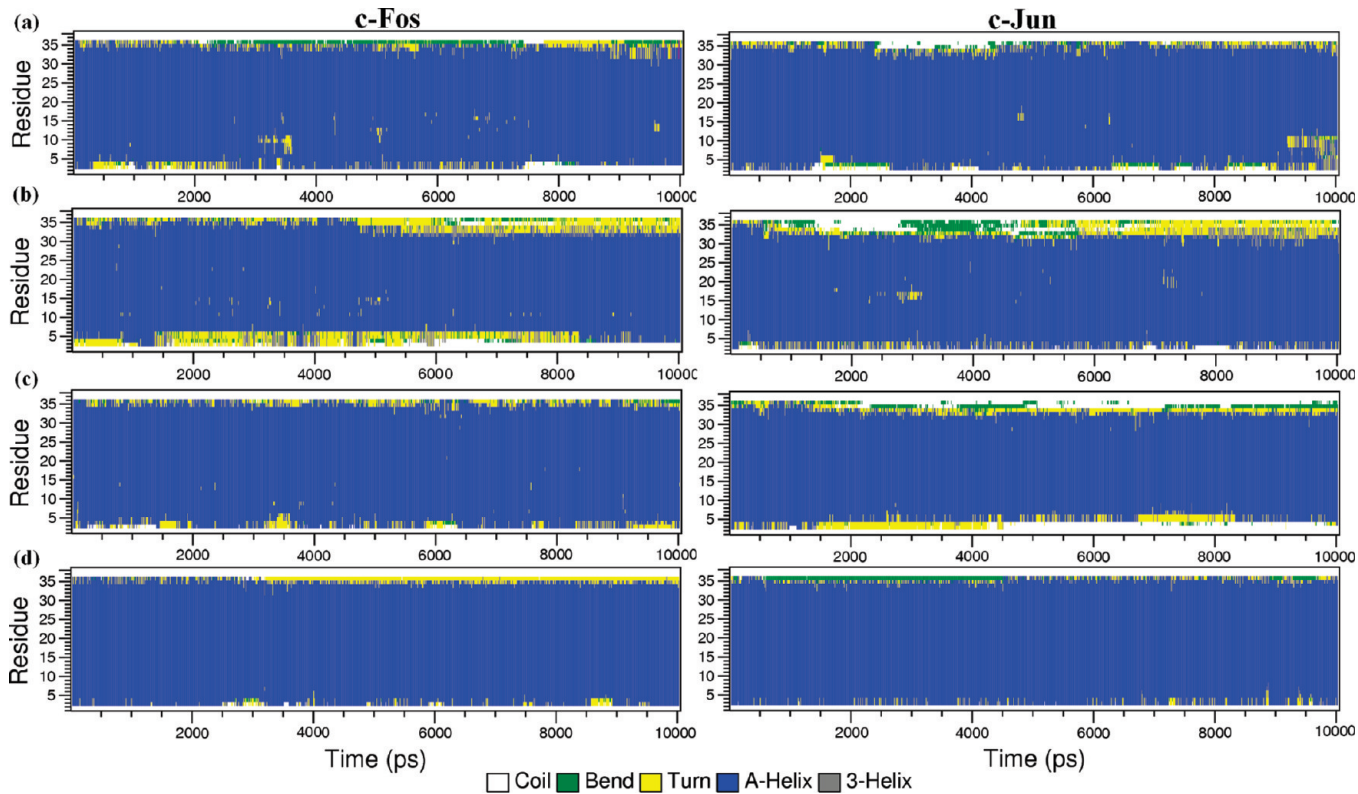


Figure 3. Time evolution of the secondary structure profile of the c-Fos–c-Jun coiled coil complex in single-trajectory approach simulations with the following combinations of protein force fields and water potentials: (a) ff99SB/TIP3P, (b) ff99SB/TIP4P, (c) ff99SB/TIP4P-Ew, and (d) ff02/POL3. The plots on the left-hand side are for c-Fos, and those on the right-hand side are for c-Jun.

protein were lower when using the polarizable ff02/POL3 combination compared to the nonpolarizable ff99/TIP3P combination.⁵⁵

The overall stability of the c-Fos–c-Jun complex was also assessed by determining the average secondary structure conformation of the protein chains during the MD simulations using the DSSP secondary structure analysis. In the case of the single-trajectory approach simulations, the average helical propensity in the complex was estimated to be 80% (ff99SB/TIP3P), 73% (ff99SB/TIP4P), 78% (ff99SB/TIP4P-Ew), and 84% (ff02/POL3), suggesting a higher (more stable) level of secondary structure if the polarizable force field and the water potential combination are used. The corresponding time evolution of the secondary structure profiles can be seen in Figure 3. The coiled coil structure obtained with the ff02/POL3 combination has the highest α -helical content in nearly all amino acids, except for a few residues in the C-terminus. In the case of the nonpolarizable protein force field/water potential combinations, while most amino acids retained an α -helical conformation, those amino acids in either or both termini were seen to have either ‘turn’ or ‘bend’ conformations at various stages during the simulations, as seen in Figure 3. For example, in the simulation with the ff99SB/TIP4P combination, amino acids in both termini of c-Fos and in the C-terminus of c-Jun were observed primarily in a ‘turn’ conformation, suggesting that the C-termini are less stable. In the simulation with the ff99SB/TIP3P combination the conformation of approximately 10 amino acids near the N-terminus of c-Jun was seen at times to change into the ‘turn’ conformation.

In the case of the multiple short-trajectory approach simulations, the average helical propensity of all the amino

acids in the complex was estimated to be 83% (ff99SB/TIP3P), 81% (ff99SB/TIP4P), 82% (ff99SB/TIP4P-Ew), and 85% (ff02/POL3). The corresponding time evolution of the secondary structure profile (see Figure S3 in the Supporting Information) revealed that the structure of the complex did not deviate much from the starting conformation in all the protein force field/water potential combinations, as expected in shorter simulations.

Figure 4 describes the time evolution of the average rmsd and the total α -helicity of the c-Fos–c-Jun complex in single-trajectory approach simulations for each force fields/water potential combination. A weak correlation can be seen between large fluctuations of secondary structure and average rmsd. In particular, long-lasting increases in rmsd tend to correlate with periods of decreased helicity. This suggests that decreased stability, as measured by a higher average rmsd of the coiled coil complex, tends to correspond to a decrease in total α -helicity.

The rmsd and α -helicity analyses have shown that both peptides in the c-Fos–c-Jun complex remain relatively stable during the single-trajectory approach simulation using the ff02/POL3 combination. Figure 5 shows the time evolution of the radius gyration of the c-Fos–c-Jun complex for each force field/water potential combination. It is clear that the complex retains the lowest values of its radius of gyration in the simulation using the ff02/POL3 combination. The lower values of the radius of gyration suggest that the interaction between the c-Fos and c-Jun peptides leads to a tighter complex in the simulation using the polarizable potentials.

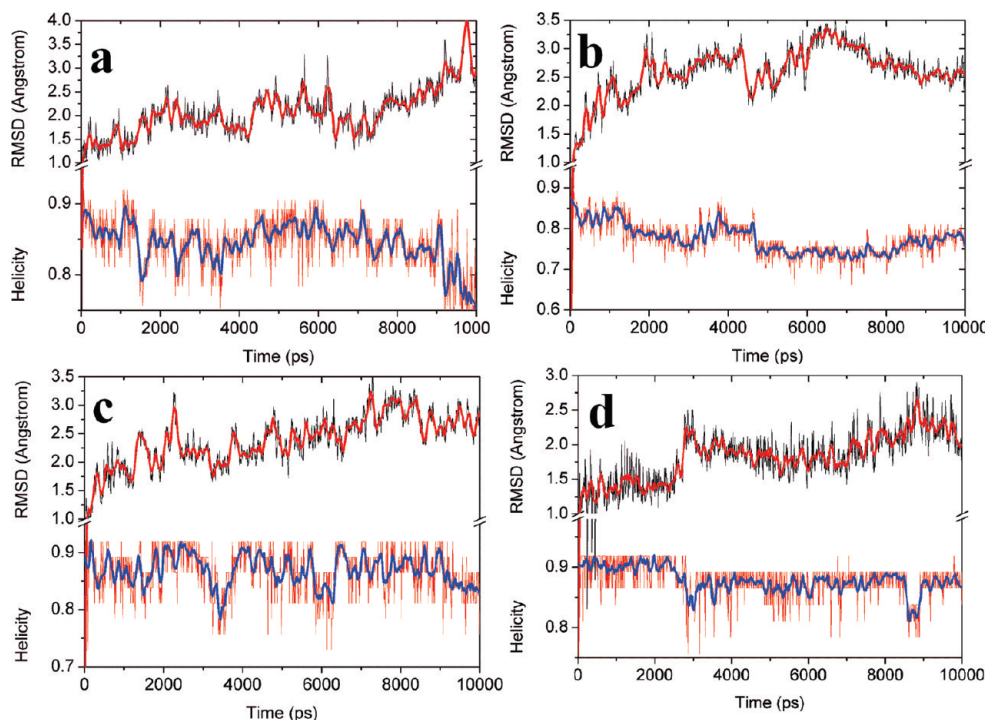


Figure 4. Time evolution of the average rmsd and the total α -helicity of the c-Fos–c-Jun coiled coil complex in single-trajectory approach simulations for each combination of protein force field and water potential: (a) ff99SB/TIP3P, (b) ff99SB/TIP4P, (c) ff99SB/TIP4P-Ew, and (d) ff02/POL3. The rmsd plot is shown with a thin black line, and the helicity plots is shown with a thin red line. Corresponding plots of averages over 200 ps intervals are shown with a thick red line for the rmsd and a thick blue line for the helicity.

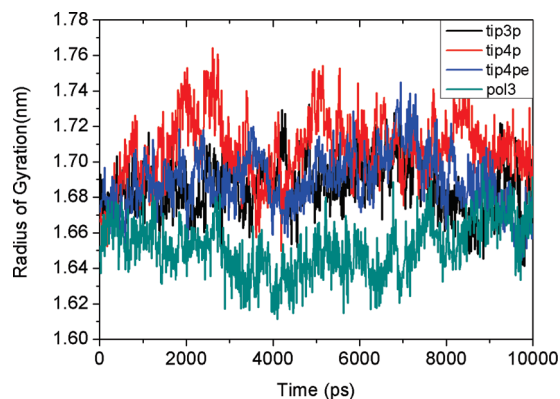


Figure 5. Time evolution of the radius of gyration during the 10.0 ns simulation of the c-Fos–c-Jun complex in the single-trajectory approach.

Structural Stability of the c-Fos and c-Jun Peptides. The c-Fos–c-Jun complex should be more stable than the individual c-Fos and c-Jun peptides during MD simulations due to stabilization of the structures through hydrophobic and hydrogen bonding interactions. The stability of the individual c-Fos and c-Jun peptides was also investigated by calculating the running average rmsd of their backbone atoms and by estimating the average secondary structure conformation using the DSSP secondary structure analysis.

As expected, the average rmsd values for the peptides in the independent-trajectory approach simulations are larger than those of the complex (single-trajectory approach) for all the nonpolarizable protein force field/water potential combinations, as shown in Table 1. The average rmsd value for the c-Fos peptide using the ff99SB/TIP3P combination is the second lowest of all combinations, while the ff99SB/TIP4P is the highest one, in agreement with the values obtained for the complex in the single-trajectory approach.

In the case of the c-Jun peptide, the average rmsd value using the ff99SB/TIP3P combination is again the second lowest, but the worst combination is now ff99SB/TIP4P-Ew. For both peptides, the polarizable ff02/POL3 combination performs significantly better than all the other combinations, as it results in the lowest rmsd values. Interestingly, the average rmsd values are in fact somewhat lower than the average rmsd value for the complex using this polarizable combination. These observations are also related to the fact that both peptides appear to be relatively more stable and retain their α -helical conformation with only a small proportion of ‘turns’ or ‘3-helical’ regions at only one terminus of each peptide: the N-terminus for the c-Jun peptide and C-terminus for the c-Fos peptide (see below).

The DSSP secondary structure analysis revealed that the average helical propensity of all amino acids during the independent-trajectory approach simulations was 72% (ff99SB/TIP3P), 48% (ff99SB/TIP4P), 61% (ff99SB/TIP4P-Ew), and 84% (ff02/POL3) for c-Fos and 54% (ff99SB/TIP3P), 58% (ff99SB/TIP4P), 50% (ff99SB/TIP4P-Ew), and 84% (ff02/POL3) for c-Jun. These results reveal that the polarizable ff02/POL3 combination again results in the most stable conformations of these peptides, while the other nonpolarizable combinations result in substantial decreases in helical propensity. The corresponding time evolution of the secondary structure profiles can be seen in Figure 6. It can be seen that the simulations using the nonpolarizable combinations result in repeated changes from α -helical to turn and bend conformations all along the peptide chains.

We would like to point out that increased structural stability when using polarizable water potentials should not be unexpected. Polarizable water potentials treat electrostatic dipole moments in such a way that they can adapt to instantaneous water configurations. Consequently the hydra-

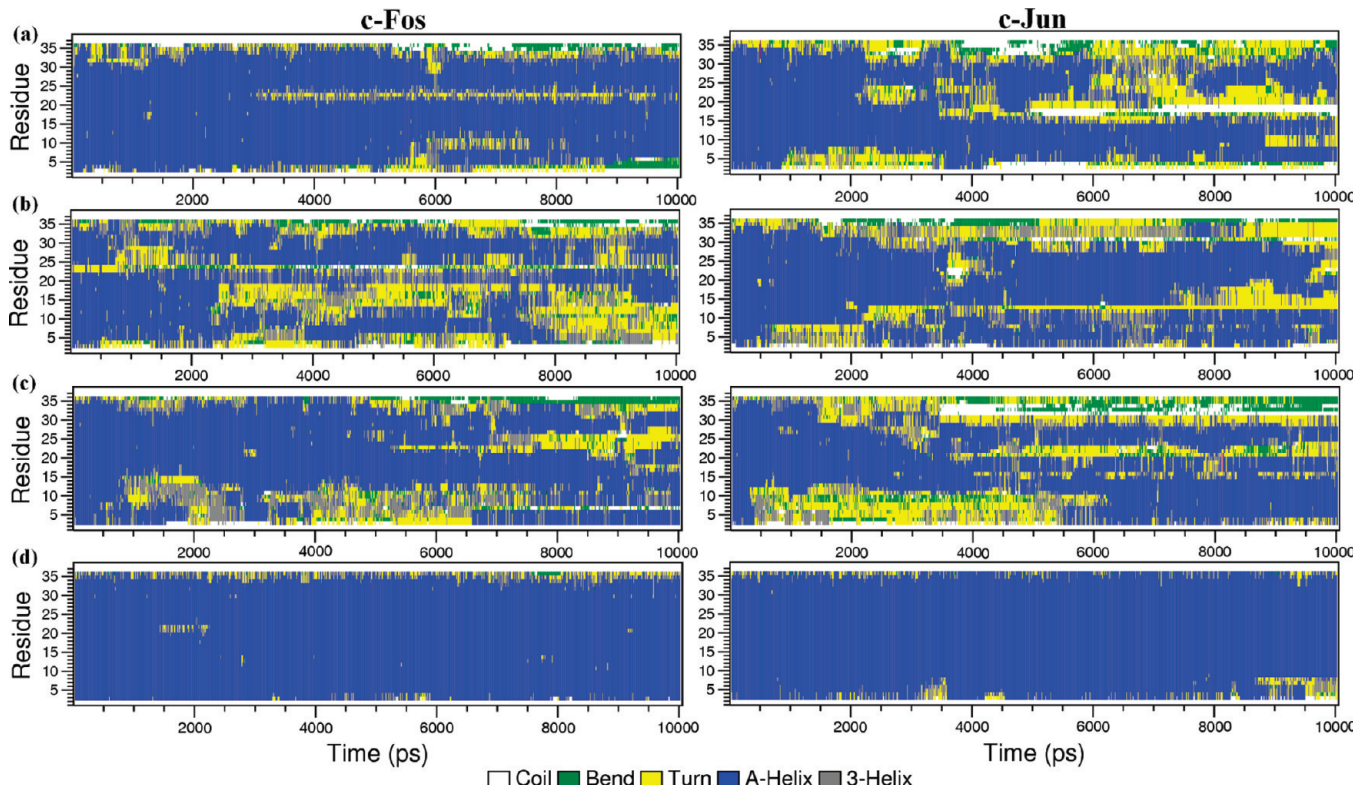


Figure 6. Time evolution of the secondary structure profiles of the c-Fos and c-Jun proteins in independent-trajectory approach simulations with the following combinations of protein force fields and water potentials: (a) ff99SB/TIP3P, (b) ff99SB/TIP4P, (c) ff99SB/TIP4P-Ew, and (d) ff02/POL3. The plots on the left-hand side are for c-Fos, and those on the right-hand side are for c-Jun.

Table 2. Free Energy of Binding Contributions (in kJ/mol) in the Single-Trajectory Approach

force field/water potential	ΔE_{ele}	ΔE_{vdw}	ΔE_{int}	ΔG_{pbss}	ΔG_{gbsa}	$\Delta G_{\text{mmppbsa}}$	ΔG_{mmgbsa}	$T\Delta S$	$\Delta G_{\text{bind-pb}}$	$\Delta G_{\text{bind-gb}}$
ff99SB/TIP3P	-1386.5	-344.9	0.0	1436.7	1476.4	-295.1	-255.4	-227.0	-68.1	-28.4
ff99SB/TIP4P	-1507.7	-375.4	0.0	1601.4	1622.3	-282.2	-260.8	-223.6	-58.5	-37.2
ff99SB/TIP4P-Ew	-1495.2	-392.5	0.0	1575.0	1608.0	-312.7	-280.1	-240.8	-71.9	-39.3
ff02/POL3	-1673.7	-347.8	0.0	1689.1	1756.0	-332.3	-265.4	-216.1	-116.2	-49.3

tion ability of polarizable water tends to be smaller than that of water treated with a pairwise additive potential. Earlier studies using polarizable potentials have shown a reduction of the acetate hydration number⁵⁶ and the carboxylate hydration numbers in charged amino acids.^{57,58} Similar structural stability was observed in relation to a smaller rmsd of the backbone atoms of thioredoxin when using polarizable force fields compared to nonpolarizable force fields in MD simulations.⁵⁹ The effect of polarization on the hydration properties of water might thus indeed account for the observed higher structural stability of proteins and peptides, resulting in an apparent increased intermolecular interaction in the absence of stronger interactions with water.

Free Energy of Binding of the c-Fos–c-Jun Complex. Calculation of the free energy of binding of the c-Fos–c-Jun complex provided a thermodynamic measure of the strength of the interaction between the two peptides. The single-trajectory approach (where only the simulation of the protein complex is carried out, and the coordinates and free energies of each protein are extracted directly from the complex) has been widely used in many MM/PB(GB)SA studies to reduce simulation times and take advantage of the likely cancellation of errors in the internal energies of the interacting molecules, resulting in relatively accurate predic-

tions of free energies of binding.^{60–62} On the other hand, the independent-trajectory approach (where three simulations are carried out: the complex and each protein separately) is able to take into account changes in intramolecular energies arising from induced fit effects, resulting in more realistic simulations of the process of interaction. However, this approach can give less accurate predictions due to large changes in the computed free energies that do not cancel out effectively. Alternatively, averaging over multiple single-trajectories may have the additional advantage of improved accuracy through an enhancement in the exploration of conformational phase space in cases where there are limited conformational changes upon the interaction of two protein molecules. In order to determine which approach is the most appropriate for the prediction of the free energy of binding between the c-Fos and c-Jun peptides in their coiled coil complex, MM/PB(GB)SA calculations were carried out using these three approaches.

Table 2 shows the predicted free energy of binding and its various components using the single-trajectory approach for all the force field/water potential combinations. When using the MM/PBSA method, the highest (least favorable) free energy of binding (-58.5 kJ/mol) was obtained with the ff99SB/TIP4P combination, while the lowest (most

Table 3. Free Energy of Binding Contributions (in kJ/mol) in the Multiple Short-Trajectory Approach^a

force field/water potential	ΔE_{ele}	ΔE_{vdw}	ΔE_{int}	ΔG_{pbsa}	ΔG_{gbsa}	ΔG_{mmpbsa}	ΔG_{mmgbsa}	$T\Delta S$	$\Delta G_{bind-pb}/STD$	$\Delta G_{bind-gb}/STD$
ff99SB/TIP3P	-1507.7	-385.8	0.0	1566.2	1610.1	-327.3	-283.4	-235.8	-91.5/8.0	-47.7/6.2
ff99SB/TIP4P	-1589.7	-382.5	0.0	1654.9	1693.7	-316.8	-278.4	-236.2	-80.7/8.3	-42.2/6.5
ff99SB/TIP4P-Ew	-1607.2	-383.7	0.0	1679.9	1715.9	-311.0	-275.0	-230.3	-80.7/8.7	-44.7/6.8
ff02/POL3	-1672.4	-374.1	0.0	1707.9	1770.6	-338.6	-275.5	-222.0	-116.6/7.9	-53.5/6.1

^a STD indicates standard deviation.

Table 4. Free Energy of Binding Contributions (in kJ/mol) in the Independent-Trajectory Approach

force field/water potential	ΔE_{ele}	ΔE_{vdw}	ΔE_{int}	ΔG_{pbsa}	ΔG_{gbsa}	ΔG_{mmpbsa}	ΔG_{mmgbsa}	$T\Delta S$	$\Delta G_{bind-pb}$	$\Delta G_{bind-gb}$
ff99SB/TIP3P	-1475.1	-438.1	53.9	1440.0	1496.0	-419.7	-362.8	-218.2	-201.5	-144.6
ff99SB/TIP4P	-1059.6	-457.7	64.4	1104.8	1147.4	-348.2	-306.0	-188.5	-159.7	-117.5
ff99SB/TIP4P-Ew	-1346.8	-517.9	83.6	1333.8	1386.1	-447.7	-395.0	-202.3	-245.4	-192.7
ff02/POL3	-1538.7	-365.8	29.3	1574.6	1631.0	-300.5	-243.7	-215.7	-84.9	-28.0

favorable) free energy of binding (-116.6 kJ/mol) was obtained with the ff02/POL3 combination. When using the MM/GBSA method, the highest free energy of binding (-28.4 kJ/mol) was obtained with the ff99SB/TIP3P combination, while the lowest free energy of binding (-49.3 kJ/mol) was again obtained with the ff02/POL3 combination. Overall, the predicted values of the free energy of binding with the MM/GBSA method were higher than those predicted with the MM/PBSA method. While calculations with the MM/GBSA method using the ff02/POL3 combination also resulted in the lowest free energy of binding, this was only possible because of a small vibrational entropy component. The apparent lack of consistent ‘ranking’ of the free energies of binding using the nonpolarizable force field/water potential combinations between the two methods may simply be due to the smaller (less reliable) differences in the free energies of binding computed using the MM/GBSA method. It nonetheless appears that using the ff02 polarizable force field and POL3 water potential consistently result in lower estimates of the free energy of binding of the c-Jun-c-Fos complex.

Table 3 shows the predicted free energies of binding and its various components using the multiple short-trajectory approach for all the force field/water potential combinations. A comparison of the values in Tables 2 and 3 reveals that the predicted free energies of binding are more negative in all force field/water potential combinations using the multiple short-trajectory approach, with the ff02/POL3 combination still producing the lowest values. This suggests that the multiple short-trajectory approach results in lower predicted free energies of binding, mostly as a consequence of stronger electrostatic interactions (by 50–84 kJ/mol), although this does not appear to be the case with the polarizable ff02/POL3 combination, where the contribution to the free energy of binding arising from electrostatic interactions is largely unaffected. Calculations using the MM/PBSA method show that the highest free energies of binding were obtained with both the ff99SB/TIP4P and ff99SB/TIP4P-Ew combinations (the values are very similar), with good relative agreement with the ranking of free energies of binding obtained with the MM/GBSA method. However, the free energies of binding obtained with the MM/PBSA method are lower by about 37–63 kJ/mol, depending on the force field/water potential combination, although again this is not the case

with the polarizable ff02/POL3 combination, with which the free energies of binding remain nearly the same.

Table 4 reports the predicted free energies of binding and its various components using the independent-trajectory approach for all force field/water potential combinations. The reported values are significantly different to their corresponding counterparts in Tables 2 and 3. The first difference to note is that the free energies of binding calculated with the polarizable ff02/POL3 combination are now the highest (least stable) for all force fields, for both MM/PBSA (-84.4 kJ/mol) and MM/GBSA (-28.0 kJ/mol) methods, with increases of approximately 25–33 kJ/mol with respect to the values obtained with the other simulation approaches (Tables 2 and 3). Nonetheless, use of the other (nonpolarizable) force field/water potential combinations resulted in large decreases in the predicted free energies of binding. The lowest free energies of binding were now obtained with the ff99SB/TIP4P-Ew combination with both the MM/PBSA (-245.4 kJ/mol) and MM/GBSA (-192.7 kJ/mol) methods, with clear increases of approximately 167 kJ/mol with respect to the values obtained with the other simulation approaches. In the case of the other nonpolarizable ff99SB/TIP3P and ff99SB/TIP4P combinations, the predicted free energies of binding decrease by about 85–125 kJ/mol for both solvation methods. A comparison of the free energy contributions reported in Tables 2–4 reveals that these large free energy changes resulted from more negative van der Waals energy changes (ΔE_{vdw}) and less positive solvation free energy changes (ΔG_{pbsa} and ΔG_{gbsa}). The additional positive contributions to the free energy from changes to the internal potential energies (ΔE_{int}) are not large enough to compensate these increases. However, these larger free energy contributions in fact arise from a lack of stability of the peptides. As discussed in the previous section, simulations of each peptide on its own using any of the nonpolarizable force field/water potential combinations resulted in large increases in their average rmsd and in significant decreases of their helical propensity. This is accompanied by larger changes to the van der Waals and electrostatic energies of the peptides with respect to their conformation in the complex, resulting in much larger and more favorable contributions to the free energy of binding. Hence the lack of structural stability of the peptides in solution gives the (wrong) impression that the lower free energies of binding result arise from stronger

Table 5. Average Closest Interhelical Distances (\AA) between Heteroatoms in Charged Groups in Amino Acids (Lys, Arg, Glu, and Asp) at Positions *e* and *g* on Different Peptides in Single-Trajectory Approach Simulations

force field/water potential	single-trajectory		
	E168-K297	D174-K292	E182-R311
ff99SB/TIP3P	6.5	7.9	4.8
ff99SB/TIP4P	9.9	5.0	5.5
ff99SB/TIP4P-Ew	7.4	5.7	5.1
ff02/POL3	5.1	5.2	4.4
experiment (PDB 1FOS)	3.1	3.0	3.3

interactions in the independent-trajectory approach. In the case of the polarizable ff02/POL3 combination, the peptides remain stable (and hence closer to their structure in the complex) throughout their independent simulations, resulting in comparatively smaller free energies of binding.

The free energy of interaction of DNA–small molecule calculated by the MM/PBSA method has also been found to be overestimated using either polarizable or nonpolarizable force fields in single-trajectory simulations. The binding energies calculated from the single-trajectory approach MD simulation were -217.8 and -320.2 kJ/mol for the polarizable and nonpolarizable force fields, respectively, which are overestimates of the experimental value of -42.6 kJ/mol (determined by isothermal titration calorimetry). For the independent-trajectory approach, the nonpolarizable force field yielded a value of -194.4 kJ/mol, which is still an overestimation, while the polarizable force field provided a value of -64.4 kJ/mol, much closer to the experimental value.³³

Earlier reports in the literature have stated that the stability of α -helical coiled coil peptides arises mainly from electrostatic and hydrophobic interactions as well as entropic contributions.^{14,63,64} In this study, the interaction between the two peptides appears to be dominated primarily by electrostatic interactions, followed by van der Waals interactions and entropic contributions. For example, the free energy contributions computed in the simulation using the ff02/POL3 combination with the independent-trajectory approach are $\Delta E_{\text{ele}} = -1538.7$ and $\Delta E_{\text{vdw}} = -365.8$ kJ/mol.

Since electrostatic interactions appear to be the dominant force driving the binding of the two peptides in their coiled coil complex, ionic interactions between oppositely charged residues in positions *e* or *g* on one peptide and *e'* or *g'* on the other one are of particular importance. Table 5 reports the average interhelical distances between the heteroatoms (N in NH_3^+ and O in COO^- , as illustrated in Figure 7) in the charged groups of amino acids at the *e*, *g* and/or *e'*, *g'* positions. The average distances were calculated from snapshots taken every 10 ps over 10.0 ns for each force field/water potential combination in the single-trajectory approach simulations. Figure 7 illustrates the three pairs of charged residues that were considered: Glu168–Lys297, Asp174–Lys292, and Glu182–Arg311. The average distances obtained from all the MD simulation trajectories are larger than those found in the crystal structure (PDB code 1FOS), suggesting a possible weakening of the coiled coil structure in the simulation. The average distances computed from the simulation using the ff02/POL3 combination are the closest to the experimental values, in agreement with the above-reported values of the rmsd and free energies of binding,

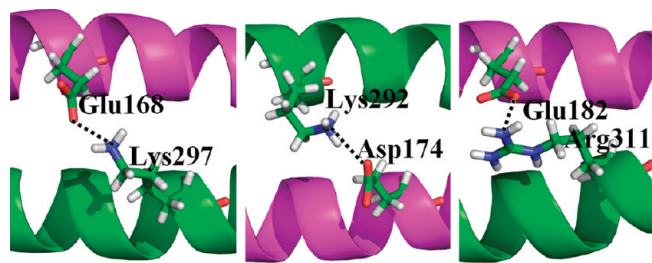


Figure 7. Pairs of charged residues at the *e*, *g* and/or *e'*, *g'* positions. The helix colored in magenta is the c-Fos peptide, and the helix colored in green is the c-Jun peptide. The dash line indicates the ionic interaction between the heteroatoms in the two charged groups.

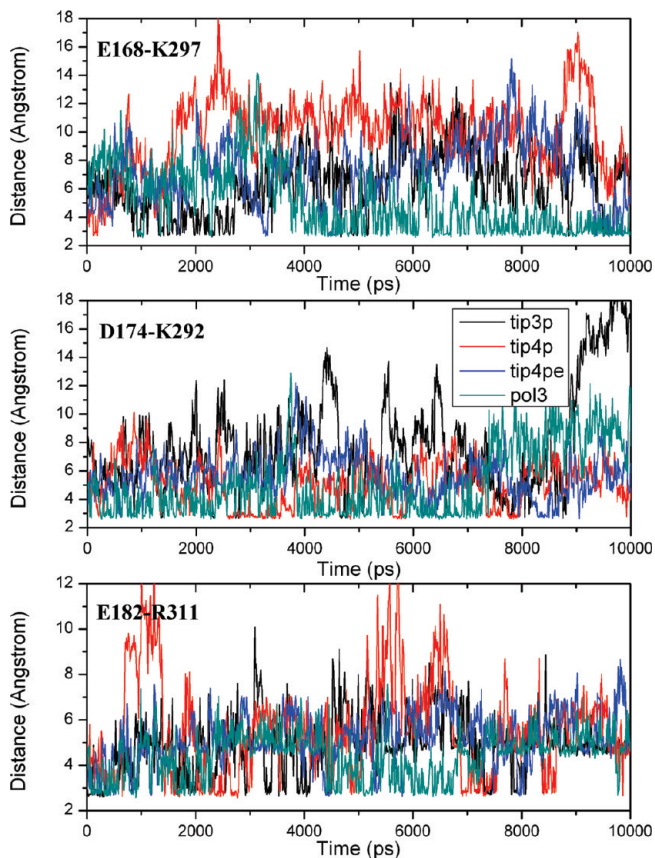


Figure 8. Time-dependent evolution of the interatomic distances between the heteroatoms (N in NH_3^+ and O in COO^-) in the charged groups of amino acids at the *e*, *g* and/or *e'*, *g'* positions. From the top, the figures correspond to the Glu168–Lys297, Asp174–Lys292, and Glu182–Arg311 pairs. Each line corresponds to a different water potential: TIP3P (black), TIP4P (red), TIP4P-Ew (blue), and POL3 (green).

suggesting that the lower free energy using this force field/water potential combination represents greater thermodynamic stability. Plots of the time evolution of the interatomic distance between the heteroatoms in these charged amino acid pairs are shown in Figure 8. It can be seen that, in general, smaller fluctuations of the interatomic distances as measured during the simulations are obtained when using the ff02/POL3 combination, which re-enforces the picture of increased stability of the complex. It can be concluded that the ionic interactions between residues in positions *e* or *g* on one peptide and *e'* or *g'* on the other play a key role in the stability and the affinity between c-Jun and c-Fos peptides in their coiled coil complex.

The experimental value of the free energy of binding of the c-Fos–c-Jun complex is -17.1 kJ/mol , which was obtained through determinations of the melting temperature (T_m) using circular dichroism measurements.¹¹ All of our predictions using the MM/PB(GB)SA method overestimate the affinity of binding. Similar studies using the MM/PBSA method have been reported where the free energies of binding have been overestimated by about 41.8 kJ/mol for coiled coil systems.^{14,63} The reason of this overestimation is still not clear, but it may be explained, at least in part, by the fact that experimental determinations of the free energy of binding measure not only the dissociation of the two peptides but also the partial unfolding of each peptide during unbinding as the temperature is increased. Both processes occur at the same time, and their contributions to the free energy of binding are difficult to disentangle, although the peptides unfold to a small extent in the independent-trajectory approach. On the other hand, MD simulations can separate both processes, but MM/PB(GB)SA calculations do not take into account any unfolding of the peptides.

Clearly, simulations using the single-trajectory approach give the best agreement with experiment, with the MM/GBSA method giving better agreement than the MM/PBSA method. The closest agreement is obtained using the ff99SB/TIP3P combination, with a predicted the free energy of binding of -28.0 kJ/mol . However, we have observed that the use of the polarizable ff02/POL3 combination results in significantly more stable structures, making these simulations more reliable. The predicted free energy of binding with the ff02/POL3 combination is -49.3 kJ/mol .

The c-Fos–c-Jun coiled coil complex appears to have higher intrinsic flexibility at the terminal portions of the peptide helices, which constitutes an additional source of error in MM/PB(GB)SA calculations.¹⁴ Hence, it would appear that simulations using the MM/PB(GB)SA method should consider only the central portions of the helices and disregard a number of terminal residues in the computation of the various contributions to the free energy. It has been reported that the magnitude of the various components of the energy of interaction of α -helical coiled coils is dependent on the choice of force field and the number of residues in the α -helix in each monomer (which preferably should be no more than 16), as otherwise the conformation of terminal residues is not stable during MD simulations.^{15,16} This study confirms that simulations using the polarizable ff02 force field and POL3 water potential result in more stable coiled coil structures and that the secondary structure of terminal residues of peptides as long as 39 residues remains stable during the time scale (10 ns) of the simulations.

Overall, the ff02/POL3 combination performs consistently better, resulting in the lowest average backbone rmsd values and the most stable secondary structures of the peptides. Importantly, in relation to the MM/PB(GB)SA calculations, the free energy of binding estimated from simulations did not change as much as with the other nonpolarizable force field and water potential combinations in the various simulation approaches (single-trajectory, multiple short-trajectory and independent-trajectory). In the case of the independent-trajectory approach, the free energy of binding is more accurately predicted compared to the experimental value.

Additive force fields have undeniably had many successes in predicting binding affinities. However, in a high-dielectric

solvent, such as water, biomolecular systems will have a strong polarizing effect, affecting the predicted geometry and thermodynamics of molecular recognition. The effect of electronic polarization has been found to be crucial in the calculation of protein–ligand binding free energies,⁶⁵ where the polarization energy has been determined to always make a negative (stabilizing) contribution to total energy. Polarizable charges have been found to give a more realistic charge redistribution between amino acids in proteins.³¹ Protein conformations as simulated using a polarizable force field in combination with the POL3 water potential were deemed to be more consistent with NMR and CD experimental data.³⁹ It thus appears that the ff02/POL3 combination can be used to provide the most reliable conformations and consistent estimates of the free energy of binding of coiled coil complexes with the MM/PB(GB)SA method. This method may provide a quick and reliable way of estimating the relative binding affinity of different coiled coil complexes, even if their absolute free energies of binding are not accurately predicted. Regardless of the additional computational expense, polarizable force fields and potentials can be used in protein, protein–protein complex, and protein–ligand complex simulations to study their structural, dynamic, and recognition properties.

CONCLUSIONS

We have investigated how the choice of solvation model and the polarization effects influence the stability, structure, and prediction of the free energy of binding of coiled coil protein complexes in MD simulations of the c-Fos–c-Jun complex. We have also investigated the effect of using different simulation approaches in MM/PB(GB)SA free energy calculations, including the single-, independent-, and multiple-trajectory approaches. The AMBER polarizable (ff02) and nonpolarizable (ff99SB) force fields in combination with the nonpolarizable TIP3P, TIP4P, and TIP4P_Ewald and the polarizable POL3 water potentials were considered.

The polarizable force field ff02 and POL3 water potential combination has been found to be better for maintaining the structural stability of the c-Fos–c-Jun complex during MD simulations. Computation of the average rmsd, helicity, and secondary structure profile analysis all consistently showed that the structure of the peptides is preserved with this force field/water potential combination. The largest component of the free energy of binding can be attributed to the electrostatic interactions in the coiled coil complex, which can be traced to specific ionic interactions between charged residues at e , g , e' , and g' positions. These interactions are maintained to a larger extent with the ff02/POL3 combination than with the nonpolarizable combinations. Consequently we conclude that predictions of the free energy of binding should be carried out using this combination. Use of the GB solvation model, as opposed to the PB solvation model, resulted consistently in values of the free energy of binding that are closer to the experimental value, for both nonpolarizable and polarizable force field and water potential combinations. However, all calculations using the MM/PB(GB)SA method overestimated the free energy of binding. Nonetheless, this approach is likely to be reliable for the calculation of relative free energies of binding, for example, when comparing the binding affinities of different peptides to the same peptide/protein partner.

Supporting Information Available: Some rmsd analysis data and secondary structure analysis results are available as supporting figures. This information is available free of charge via the Internet at <http://pubs.acs.org/>.

REFERENCES AND NOTES

- (1) Gerrard, J. A.; Hutton, C. A.; Perugini, M. A. Inhibiting protein-protein interactions as an emerging paradigm for drug discovery. *Mini-Rev. Med. Chem.* **2007**, *7*, 151–157.
- (2) Kumar, R.; Thompson, E. B. Gene regulation by the glucocorticoid receptor: structure:function relationship. *J. Steroid Biochem. Mol. Biol.* **2005**, *94*, 383–394.
- (3) Bjurlin, M. A.; Byron, K. L. Protein-protein interactions in vasopressin signal transduction: new evidence for cytoskeletal dynamics. *J. Am. Osteopath. Assoc.* **2005**, *105*, 24–25.
- (4) Selvakumar, P.; Sharma, R. K. Role of calpain and caspase system in the regulation of N-myristoyltransferase in human colon cancer (Review). *Int. J. Mol. Med.* **2007**, *19*, 823–827.
- (5) Lee, J. W.; Harrigan, J.; Opresko, P. L.; Bohr, V. A. Pathways and functions of the Werner syndrome protein. *Mech. Ageing Dev.* **2005**, *126*, 79–86.
- (6) Wolf, E.; Kim, P. S.; Berger, B. MultiCoil: a program for predicting two- and three-stranded coiled coils. *Protein Sci.* **1997**, *6*, 1179–1189.
- (7) Landschulz, W. H.; Johnson, P. F.; McKnight, S. L. The leucine zipper: a hypothetical structure common to a new class of DNA binding proteins. *Science* **1988**, *240*, 1759–1764.
- (8) O’Shea, E. K.; Lumb, K. J.; Kim, P. S. Peptide ‘Velcro’: design of a heterodimeric coiled coil. *Curr. Biol.* **1993**, *3*, 658–667.
- (9) Graddis, T. J.; Myszka, D. G.; Chaiken, I. M. Controlled formation of model homo- and heterodimer coiled coil polypeptides. *Biochemistry* **1993**, *32*, 12664–12671.
- (10) Bornschlogl, T.; Rief, M. Single-molecule dynamics of mechanical coiled coil unzipping. *Langmuir* **2008**, *24*, 1338–1342.
- (11) Mason, J. M.; Schmitz, M. A.; Muller, K. M.; Arndt, K. M. Semirational design of Jun-Fos coiled coils with increased affinity: Universal implications for leucine zipper prediction and design. *Proc. Nat. Acad. Sci. U.S.A.* **2006**, *103*, 8989–8994.
- (12) Hagemann, U. B.; Mason, J. M.; Muller, K. M.; Arndt, K. M. Selectional and mutational scope of peptides sequestering the Jun-Fos coiled coil domain. *J. Mol. Biol.* **2008**, *381*, 73–88.
- (13) Grigoryan, G.; Reinke, A. W.; Keating, A. E. Design of protein-interaction specificity gives selective bZIP-binding peptides. *Nature* **2009**, *458*, 859–864.
- (14) Salwiczek, M.; Samsonov, S.; Vagt, T.; Nyakatura, E.; Fleige, E.; Numata, J.; Cölfen, H.; Pisabarro, M. T.; Koksch, B. Position-Dependent Effects of Fluorinated Amino Acids on the Hydrophobic Core Formation of a Heterodimeric Coiled Coil. *Chem.—Eur. J.* **2009**, *15*, 7628–7636.
- (15) Pendley, S. S.; Yu, Y. B.; Thomas, E.; Cheatham, I. Molecular dynamics guided study of salt bridge length dependence in both fluorinated and non-fluorinated parallel dimeric coiled coils. *Proteins: Struct., Funct., Bioinf.* **2009**, *74*, 612–629.
- (16) Lee, H.; Larson, R. G. Prediction of the stability of coiled coils using molecular dynamics simulations. *Mol. Simul.* **2007**, *33*, 463–473.
- (17) Best, R. B.; Hummer, G. Optimized molecular dynamics force fields applied to the helix-coil transition of polypeptides. *J. Phys. Chem. B* **2009**, *113*, 9004–9015.
- (18) Jouaux, E. M.; Timm, B. B.; Arndt, K. M.; Exner, T. E. Improving the interaction of Myc-interfering peptides with Myc using molecular dynamics simulations. *J. Pept. Sci.* **2009**, *15*, 5–15.
- (19) Aqvist, J.; Medina, C.; Samuelsson, J. E. A new method for predicting binding affinity in computer-aided drug design. *Protein Eng.* **1994**, *7*, 385–391.
- (20) Perdih, A.; Bren, U.; Solmajer, T. Binding free energy calculations of N-sulphonyl-glutamic acid inhibitors of MurD ligase. *J. Mol. Model.* **2009**, *15*, 983–996.
- (21) Lee, F. S.; Chu, Z. T.; Bolger, M. B.; Warshel, A. Calculations of antibody-antigen interactions: microscopic and semi-microscopic evaluation of the free energies of binding of phosphorylcholine analogs to McPC603. *Protein Eng.* **1992**, *5*, 215–228.
- (22) Bren, U.; Lah, J.; Bren, M.; Martinek, V.; Florian, J. DNA duplex stability: the role of preorganized electrostatics. *J. Phys. Chem. B* **2010**, *114*, 2876–2885.
- (23) Kuhn, B.; Kollman, P. A. A Ligand That Is Predicted to Bind Better to Avidin than Biotin: Insights from Computational Fluorine Scanning. *J. Am. Chem. Soc.* **2000**, *122*, 3909–3916.
- (24) Chong, L. T.; Duan, Y.; Wang, L.; Massova, I.; Kollman, P. A. Molecular dynamics and free-energy calculations applied to affinity maturation in antibody 4G7. *Proc. Nat. Acad. Sci. U.S.A.* **1999**, *96*, 14330–14335.
- (25) Huo, S.; Wang, J.; Cieplak, P.; Kollman, P. A.; Kuntz, I. D. Molecular dynamics and free energy analyses of cathepsin D-inhibitor interactions: insight into structure-based ligand design. *J. Med. Chem.* **2002**, *45*, 1412–1419.
- (26) Donini, O. A.; Kollman, P. A. Calculation and prediction of binding free energies for the matrix metalloproteinases. *J. Med. Chem.* **2000**, *43*, 4180–4188.
- (27) Gouda, H.; Kuntz, I. D.; Case, D. A.; Kollman, P. A. Free energy calculations for theophylline binding to an RNA aptamer: Comparison of MM-PBSA and thermodynamic integration methods. *Biopolymers* **2003**, *68*, 16–34.
- (28) Cui, Q.; Sulea, T.; Schrag, J. D.; Munger, C.; Hung, M. N.; Naim, M.; Cygler, M.; Purisima, E. O. Molecular dynamics-solvated interaction energy studies of protein-protein interactions: the MP1-p14 scaffolding complex. *J. Mol. Biol.* **2008**, *379*, 787–802.
- (29) Kollman, P. A.; Massova, I.; Reyes, C.; Kuhn, B.; Huo, S.; Chong, L.; Lee, M.; Lee, T.; Duan, Y.; Wang, W.; Donini, O.; Cieplak, P.; Srinivasan, J.; Case, D. A.; Cheatham, T. E. 3rd, Calculating structures and free energies of complex molecules: combining molecular mechanics and continuum models. *Acc. Chem. Res.* **2000**, *33*, 889–897.
- (30) Srinivasan, J.; Cheatham, T. E.; Cieplak, P.; Kollman, P. A.; Case, D. A.; Continuum solvent studies of the stability of DNA, R. N. A. and phosphoramidate-DNA helices. *J. Am. Chem. Soc.* **1998**, *120*, 9401–9409.
- (31) Lopes, P. E.; Roux, B.; Mackerell, A. D. Molecular modeling and dynamics studies with explicit inclusion of electronic polarizability. Theory and applications. *Theor. Chem. Acc.* **2009**, *124*, 11–28.
- (32) Halgren, T. A.; Damm, W. Polarizable force fields. *Curr. Opin. Struct. Biol.* **2001**, *11*, 236–242.
- (33) Tresewan, W.; Wittayanarakul, K.; Anthony, N. G.; Huchet, G.; Alniss, H.; Hannongbua, S.; Khalaf, A. I.; Suckling, C. J.; Parkinson, J. A.; Mackay, S. P. A detailed binding free energy study of 2:1 ligand-DNA complex formation by experiment and simulation. *Phys. Chem. Chem. Phys.* **2009**, *11*, 10682–10693.
- (34) Showalter, S. A.; Brüschweiler, R. Validation of Molecular Dynamics Simulations of Biomolecules Using NMR Spin Relaxation as Benchmarks: Application to the AMBER99SB Force Field. *J. Chem. Theory Comput.* **2007**, *3*, 961–975.
- (35) Hornak, V.; Abel, R.; Okur, A.; Strockbine, B.; Roitberg, A.; Simmerling, C. Comparison of multiple Amber force fields and development of improved protein backbone parameters. *Proteins* **2006**, *65*, 712–725.
- (36) Genheden, S.; Ryde, U. How to obtain statistically converged MM/GBSA results. *J. Comput. Chem.* **2010**, *31*, 837–846.
- (37) Case, D. A.; Cheatham III, T. E.; Darden, T.; Gohlke, H.; Luo, R.; Merz, K. M., Jr.; Onufriev, A.; Simmerling, C.; Wang, B.; Woods, R. J. The Amber biomolecular simulation programs. *J. Comput. Chem.* **2005**, *26*, 1668–1688.
- (38) Cieplak, P.; Caldwell, J.; Kollman, P. Molecular mechanical models for organic and biological systems going beyond the atom centered two body additive approximation: aqueous solution free energies of methanol and N-methyl acetamide, nucleic acid base, and amide hydrogen bonding and chloroform/water partition coefficients of the nucleic acid bases. *J. Comput. Chem.* **2001**, *22*, 1048–1057.
- (39) Wang, Z. X.; Zhang, W.; Wu, C.; Lei, H.; Cieplak, P.; Duan, Y. Strike a balance: optimization of backbone torsion parameters of AMBER polarizable force field for simulations of proteins and peptides. *J. Comput. Chem.* **2006**, *27*, 781–790.
- (40) Jorgensen, W. L.; Chandrasekhar, J.; Madura, J. D.; Impey, R. W.; Klein, M. L. Comparison of simple potential functions for simulating liquid water. *J. Chem. Phys.* **1983**, *79*, 926–936.
- (41) Hans, W. H.; William, C. S.; Jed, W. P.; Jeffry, D. M.; Thomas, J. D.; Greg, L. H.; Teresa, H.-G. Development of an improved four-site water model for biomolecular simulations: TIP4P-Ew. *J. Chem. Phys.* **2004**, *120*, 9665–9678.
- (42) Caldwell, J. W.; Kollman, P. A. Structure and Properties of Neat Liquids Using Nonadditive Molecular Dynamics: Water, Methanol, and N-Methylacetamide. *J. Phys. Chem. B* **1995**, *99*, 6208–6219.
- (43) Tom, D.; Darrin, Y.; Lee, P. Particle mesh Ewald: An N [center-dot] log(N) method for Ewald sums in large systems. *J. Chem. Phys.* **1993**, *98*, 10089–10092.
- (44) Ryckaert, J.-P.; Ciccotti, G.; Berendsen, H. J. C. Numerical integration of the cartesian equations of motion of a system with constraints: molecular dynamics of n-alkanes. *J. Comput. Phys.* **1977**, *23*, 327–341.
- (45) Berendsen, H. J. C.; Postma, J. P. M.; Gunsteren, W. F. v.; DiNola, A.; Haak, J. R. Molecular dynamics with coupling to an external bath. *J. Chem. Phys.* **1984**, *81*, 3684–3690.

- (46) Pastor, R.; Brooks, B.; Szabo, A. An analysis of the accuracy of Langevin and molecular dynamics algorithms. *Mol. Phys.* **1988**, *65*, 1409–1419.
- (47) Kabsch, W.; Sander, C. Dictionary of protein secondary structure: pattern recognition of hydrogen-bonded and geometrical features. *Biopolymers* **1983**, *22*, 2577–2637.
- (48) Bren, M.; Florián, J.; Mavri, J.; Bren, U. Do all pieces make a whole? Thiele cumulants and the free energy decomposition. *Theor. Chem. Acc.* **2007**, *117*, 535–540.
- (49) Bren, U.; Martínek, V.; Florián, J. Decomposition of the Solvation Free Energies of Deoxyribonucleoside Triphosphates Using the Free Energy Perturbation Method. *J. Phys. Chem. B* **2006**, *110*, 12782–12788.
- (50) Still, W. C.; Tempczyk, A.; Hawley, R. C.; Hendrickson, T. Semi-analytical treatment of solvation for molecular mechanics and dynamics. *J. Am. Chem. Soc.* **1990**, *112*, 6127–6129.
- (51) Sitkoff, D.; Sharp, K. A.; Honig, B. Accurate calculation of hydration free energies using macroscopic solvent models. *J. Phys. Chem.* **1994**, *98*, 1978–1988.
- (52) Sanner, M. F.; Olson, A. J.; Spehner, J.-C. Reduced surface: An efficient way to compute molecular surfaces. *Biopolymers* **1996**, *38*, 305–320.
- (53) Luo, R.; David, L.; Gilson, M. K. Accelerated Poisson-Boltzmann calculations for static and dynamic systems. *J. Comput. Chem.* **2002**, *23*, 1244–1253.
- (54) Pearlman, D. A.; Case, D. A.; Caldwell, J. W.; Ross, W. S.; Cheatham, T. E.; DeBolt, S.; Ferguson, D.; Seibel, G.; Kollman, P. AMBER, a package of computer programs for applying molecular mechanics, normal mode analysis, molecular dynamics and free energy calculations to simulate the structural and energetic properties of molecules. *Comput. Phys. Commun.* **1995**, *91*, 1–41.
- (55) Meher, B. R.; Kumar, M. V. S.; Bandyopadhyay, P. Molecular dynamics simulation of HIV-protease with polarizable and non-polarizable force fields Indian. *J. Phys. (Paris)* **2009**, *83*, 81–90.
- (56) Meng, E. C.; Kollman, P. A. Molecular Dynamics Studies of the Properties of Water around Simple Organic Solutes. *J. Phys. Chem. B* **1996**, *100*, 11460–11470.
- (57) Leung, K.; Rempe, S. B. Ab Initio Molecular Dynamics Study of Formate Ion Hydration. *J. Am. Chem. Soc.* **2003**, *126*, 344–351.
- (58) Kamiński, G. A.; Stern, H. A.; Berne, B. J.; Friesner, R. A.; Cao, Y. X.; Murphy, R. B.; Zhou, R.; Halgren, T. A. Development of a polarizable force field for proteins via ab initio quantum chemistry: first generation model and gas phase tests. *J. Comput. Chem.* **2002**, *23*, 1515–1531.
- (59) Ji, C.; Mei, Y.; Zhang, J. Z. Developing polarized protein-specific charges for protein dynamics: MD free energy calculation of pKa shifts for Asp26/Asp20 in thioredoxin. *Biophys. J.* **2008**, *95*, 1080–1088.
- (60) Liang, S.; Li, L.; Hsu, W.-L.; Pilcher, M. N.; Uversky, V.; Zhou, Y.; Dunker, A. K.; Meroueh, S. O. Exploring the Molecular Design of Protein Interaction Sites with Molecular Dynamics Simulations and Free Energy Calculations. *Biochemistry* **2008**, *48*, 399–414.
- (61) Fujiwara, S.; Amisaki, T. Identification of high affinity fatty acid binding sites on human serum albumin by MM-PBSA method. *Biophys. J.* **2008**, *94*, 95–103.
- (62) Deng, Y.; Roux, B. Computation of binding free energy with molecular dynamics and grand canonical Monte Carlo simulations. *J. Chem. Phys.* **2008**, *128*, 115103.
- (63) Orzechowski, M.; Cieplak, P.; Piela, L. Theoretical calculation of the coiled coil stability in water in the context of its possible use as a molecular rack. *J. Comput. Chem.* **2002**, *23*, 106–110.
- (64) Zhang, L.; Hermans, J. Molecular dynamics study of structure and stability of a model coiled coil. *Proteins: Struct., Funct., Genet.* **1993**, *16*, 384–392.
- (65) Jiao, D.; Golubkov, P. A.; Darden, T. A.; Ren, P. Calculation of protein-ligand binding free energy by using a polarizable potential. *Proc. Natl. Acad. Sci. U.S.A.* **2008**, *105*, 6290–6295.

CI100321H